Grass water stress estimated from phytoliths in West Africa

Laurent Bremond, Anne Alexandre, Odile Peyron, Joel Guiot

Journal of Biogeography (J. Biogeogr.) (2005) **32**, 311–327

ORIGINAL ARTICLE

Grass water stress estimated from phytoliths in West Africa

Laurent Bremond[1]*, Anne Alexandre[1], Odile Peyron[2] and Joël Guiot[1]

[1]*CEREGE, CNRS UMR 6635, Europôle Méditerranéen de l'Arbois, BP 80, F13545 Aix-en-Provence Cedex 04 and* [2]*Laboratoire de Chrono-Écologie, CNRS UMR 6565, Université de Franche-Comté UFR Sciences et Techniques, 16, Route de Gray 25030 Besançon Cedex, France*

*Correspondence: Laurent Bremond, CEREGE, CNRS UMR 6635, Europôle Méditerranéen de l'Arbois, BP 80, F13545 Aix-en-Provence Cedex 04, France.
E-mail: Bremond@cerege.fr

ABSTRACT

Aim This study calibrates the relationship between phytolith indices, modern vegetation structure, and a climate parameter (AET/PET, i.e. the ratio of annual actual evapotranspiration to annual potential evapotranspiration), in order to present new proxies for long-term Quaternary climate and vegetation changes, and model/data comparisons.

Location Sixty-two modern soil surface samples from West Africa (Mauritania and Senegal), collected along a latitudinal transect across four bioclimatic zones, were analysed.

Methods Two phytolith indices are defined as normalized data: (1) humidity-aridity index [Iph (%) = saddle vs. cross + dumbbell + saddle], and (2) water stress index [fan-shaped index (Fs) (%) = fan-shaped vs. sum of characteristic phytoliths]. Vegetation structures are delimited according to Iph and Fs boundaries. Bootstrapped regression methods are used for evaluating the strength of the relationship between the two phytolith indices and AET/PET. Additional modern phytolith assemblages, from Mexico, Cameroon and Tanzania are extracted in order to test the calibration established from the West African samples. Accuracy of the AET/PET phytolith proxy is compared with equivalent pollen proxy from the same area.

Results Characterization of the grass cover is accurately made through Iph. A boundary of 20 ± 1.4% discriminates tall grass savannas from short grass savannas. Water stress and transpiration experienced by the grass cover can be estimated through Fs. AET/PET is accurately estimated from phytoliths by a transfer function: $\mathrm{AET/PET} = -0.605\ \mathrm{Fs} - 0.387\ \mathrm{Iph} + 0.272\ (\mathrm{Iph} - 20)^2$ ($r = 0.80 \pm 0.04$) in the application domain (AET/PET ranging from 0.1 ± 0.04 to 0.45 ± 0.04). Phytolith and pollen estimate with similar precision ($r_{\mathrm{pollen}} = 0.84 \pm 0.04$) the AET/PET in the studied area.

Conclusions This study demonstrates that we can rely on the phytolith indices Iph and Fs to distinguish the different grasslands in tropical areas. Moreover, a new phytolith proxy of AET/PET, linked to water availability, is presented. We suggest from these results that combining phytolith and pollen proxies of AET/PET would help to constrain this climate parameter better, especially when phytolith assemblages are dominated by Panicoideae and Chloridoideae C_4-grass phytoliths, are devoid of Pooideae C_3-grass phytoliths, and occur with a few tropical ligneous woody dicotyledon phytoliths. As AET/PET is a bioclimatic indicator commonly used in vegetation models, such a combination would help to make model/data comparisons more efficient.

Keywords
Arid environment, grassland, palaeoclimate, palaeovegetation, phytoliths, pollen, vegetation and climate proxies, West Africa.

INTRODUCTION

Global vegetation models provide a means of translating the outputs from climate models into maps of potential vegetation distribution for present, past and future climate scenarios (Prentice *et al.*, 1992; Haxeltine & Prentice, 1996). The simplest vegetation models are based on bioclimatic indicators developed from climatic variables reflecting specific processes of plant growth or survival. These indicators, when properly chosen, are able to predict locations and potential shifts of vegetation limits in response to past or future climate change (Cramer, 2002). Examples of such indicators are growing degree days, absolute cold tolerance limits or estimates of drought stress based on a simple water balance model, i.e. the ratio of annual actual evapotranspiration to the annual potential evapotranspiration (AET/PET). Vegetation models can be coupled to climatic models to simulate past vegetation (Prentice *et al.*, 1992; Claussen & Esch, 1994) and the validity of these simulations is assessed by comparison with vegetation reconstructed from proxy data.

Phytoliths are opaline silica particles that precipitate in and/or between the cells of living plant tissues. Because of redundancy and multiplicity in phytolith shape (Rovner, 1971; Mulholland, 1989; Fredlund & Tieszen, 1994), one phytolith type can rarely be related to one plant taxon and therefore in order to use phytoliths to discern taxonomic meaning a variety of phytolith forms (the 'phytolith assemblage') must be considered. Phytolith assemblages have recently been shown to be a promising tool to discriminate between the various grasslands (Fredlund & Tieszen, 1994; Alexandre *et al.*, 1997; Barboni *et al.*, 1999). Fossil phytolith assemblages from soils, buried soils and lake sediments have been used to reconstruct palaeovegetation changes (Baker *et al.* (2000); Blinnikov *et al.* (2002); Carter 2002, and Piperno & Jones (2003)). Fossil phytolith assemblages must be interpreted in term of vegetation type, by comparison with modern assemblages collected from soil humic horizons or erosion surfaces. However, although Fredlund & Tieszen (1997) presented a calibration between phytolith assemblages and temperature for the American Great Plains, there is no advanced calibration between modern phytolith assemblages, bio-climatic data and vegetation biomes in the inter-tropical zone. The aim of this study is to fill this gap by first calibrating the relationship between phytolith indices, vegetation structure, and annual amount of growth-limiting drought stress on plants expressed by the ratio AET/PET for the West African bio-climatic zones. The resulting climate proxy is tested on a few modern phytolith assemblages from other geographical areas (Cameroon, Tanzania and Mexico) and compared with AET/PET estimated by pollen analysis for these areas.

ENVIRONMENTAL SETTING

The West African area sampled for this study ranges between 12° N (south of Senegal) and 23° N (south of Mauritania) (Fig. 1). This area is divided into four latitudinal bio-climatic zones: the Guinean zone, the Sudanian zone, the Sahelian zone and the Saharan zone (White, 1983). Climate and vegetation features of the four zones are shown in Fig. 1.

Climate

Climatic zoning is characterized from south to north by a decrease in mean annual rainfall from 1500 to 100 mm and an increase in the length of the dry season from 5 months to more than 9 months. The mean temperature of the coldest month is 25 °C in the southern region and 19 °C in the northern region. The mean temperature of the warmest month stabilizes between 30 and 31 °C.

Rainfall distribution over the area is connected to the seasonal migration of the Intertropical Convergence Zone. Three major wind systems dominate the area: the summer south-south-westerly monsoonal winds, the winter north-easterly trades winds (or Harmattan), and the summer African Easterly Jet (Ratmeyer *et al.*, 1999b; Wyputta & Grieger, 1999; Huang *et al.*, 2000).

Vegetation

The south–north rainfall gradient is reflected by the current latitudinal distribution of four major vegetation zones described by White (1983). Description of a vegetation zone is mainly based on its woody components. The only system which describes with accuracy the different tropical grasslands through continuity of the herbaceous cover, height of grasses and tree cover density is the Yangambi nomenclature (CSA, 1956). We will refer to both nomenclatures in this study. However, following the North American nomenclature, which distinguishes between short grass and tall grass prairies (Fredlund & Tieszen, 1994), we propose to use the terms 'tall grass savanna' and 'short grass savanna' in place of 'savanna' and 'steppe' as used in the Yangambi nomenclature.

Four bioclimatic zones are studied: Guinean, Sudanian, Sahelian and Saharan. Figure 1b presents the climatic patterns of the zones, the major vegetation types according to White (1983), the vegetation physiognomy and the dominant grass sub-families and genus.

The grass subfamilies that dominate in the Guinean, Sudanian and Saharan zones are considered to be similar to those that preceded human impact (Le Houérou, 1993a). However, the Sahelian zone is composed almost entirely of annual grass species and there is apparently no climatic reason why several species of perennial grasses could not thrive in this zone. One explanation for their absence is the combined effect of fire and a long, severe dry season (Le Houérou, 1993a). Perennial grass species that preceded human impact probably belonged to the same sub-family of some vestigial Panicoideae perennial grass species found in the Soudano-Sahelian subzone as defined by Le Houérou (1993a).

(a)

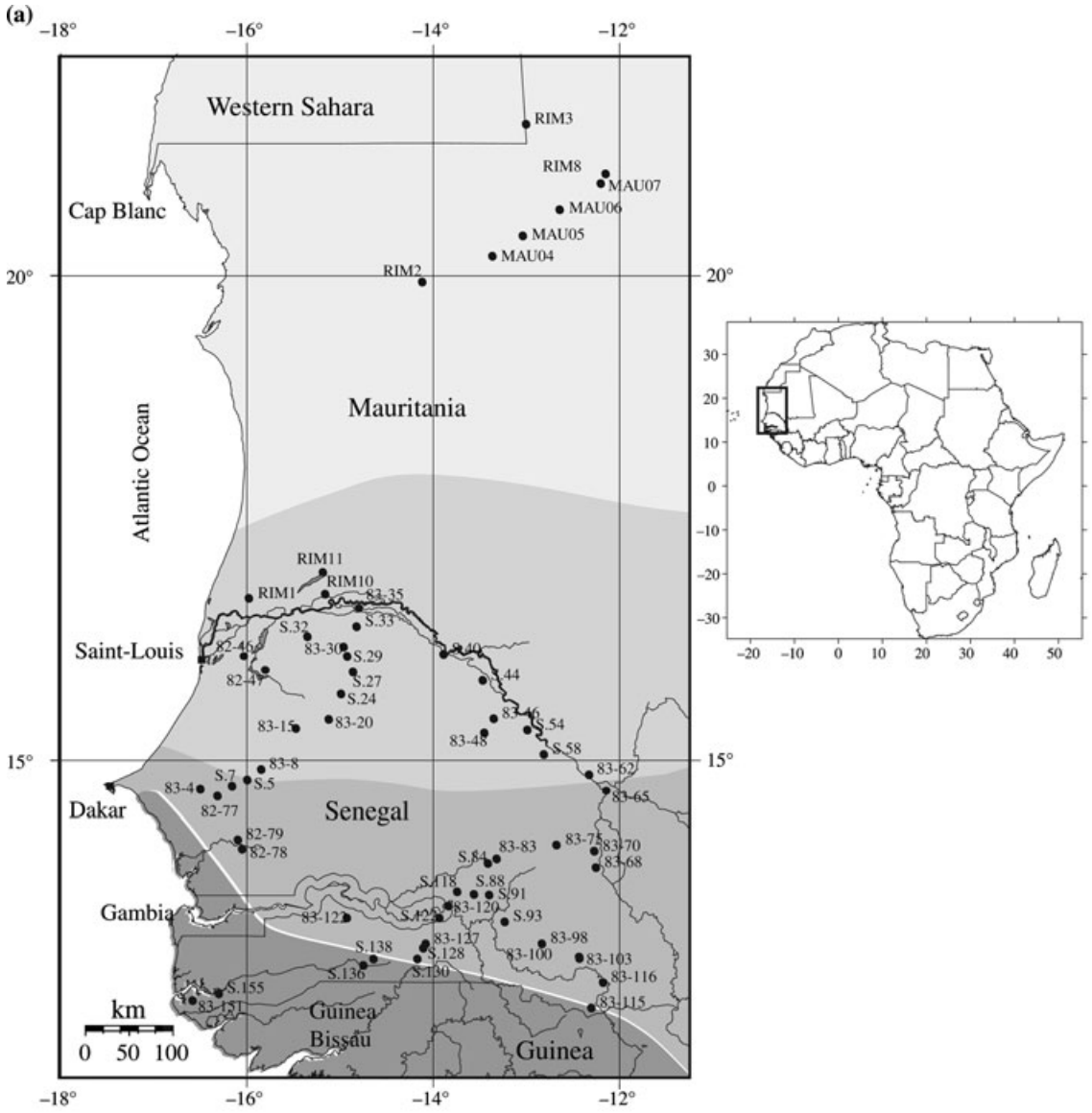

(b)

Colour Code	Bioclimatic zones according to White (1983)	Major vegetation types, according to White (1983)	Pann (mm) AET/PET	Dominant sub-family and grass species or genus, according to Wyk (1979), Lézine (1987) and Le Houérou (1993).	Vegetation physiognomy, according to the Yangamby classification (C.S.A, 1956)
	Guinean zone	Mosaic of lowland rain forest and secondary grassland	> 1000 > 0.4	*Panicoideae* perennial grasses : *Hypparenia*	Tall grass savanna Woodland Forest
	Sudanian zone	Sudanian woodland	500 – 1000 0.4 – 0.3	*Panicoideae* perennial grasses : *Andropogon, Cenchrus* Annual grasses : *Aristida, Cenchrus*	Tall grass savanna Shrub and tall-grass savanna Tree and tall grass savanna Woodland including tall grasses
	Sahelian zone	Sahel *Acacia* wooded grassland and deciduous bushland	200–500 0.3 – 0.1	*Chloridoideae* annual grasses : *Schoenefeldia, Aristida, Eragrostis*	Short grass savanna Shrub and short-grass savanna Tree and short grass savanna
	Saharan zone	Northern Sahel semi-desert grassland and shrubland Desert dunes with perennial, regs, hamadas and wadis	< 200 < 0.1	*Panicoideae* perennial grasses : *Panicum turgidum.* *Arundinoideae* annual grasses : *Aristida*	Short-grass savanna Shrub and short-grass savanna Shrub and short-grass in depressions

Figure 1 (a) Location of the samples in West Africa and main bioclimatic zones after White (1983); (b) climatic patterns and dominant grass sub-family, major vegetation types and vegetation physiognomy of the four sampled bioclimatic zones. Pann, annual precipitation (mm); AET/PET, ratio of actual evapotranspiration to potential evapotranspiration.

MATERIALS AND METHODS

Materials

Phytolith samples

Soil surface samples were collected by Anne-Marie Lézine between 1987 and 1995 during several field trips (Lézine, 1987, 1988; Lézine & Edorh, 1991; Lézine *et al.*, 1995). The sampling method consists in collecting individual sub-samples of the upper 1 cm of the soil (litter excluded), at random, over an area of *c.* 100 m^2. Sub-samples are mixed together.

Phytolith assemblages were extracted from five samples from the Guinean zone, 25 samples from the Sudanian zone, 24 samples from the Sahelian zone and nine samples from the Saharan zone (Fig. 1). Forty-three additional modern phytolith assemblages from Mexico (seven samples from the Sonoran desert), Cameroon (26 samples collected along a 750 m forest–savanna transect) and Tanzania [10 samples taken around a small crater lake (1 km in diameter)] were analysed to test the calibration established from the West African samples. Location and vegetation types of the sampled sites as well as the main characters of phytolith assemblages are summarized in Table 1.

Pollen samples

Pollen samples covered the same phytolith sampling zones, but also included several additional sampling sites. Pollen samples and data are presented in Peyron (1999).

Climate data

Mean monthly precipitation and temperature averaged over 30 years from 12 meteorological stations were obtained from the data base of Leemans & Cramer (1991) and from the Office Météo du Senegal (CSE, 2000). To evaluate the annual amount of growth-limiting drought stress on plants, we calculated the ratio between annual actual evapotranspiration and annual potential evapotranspiration (AET/PET) using a simple water balance model (Jarvis & MacNaughton, 1986; Harrison *et al.*, 1993). Required input data for calculating AET/PET are site latitude, soil water storage capacity, temperature, precipitation and sunshine. The potential evapotranspiration (a function of net radiation and temperature) is the evaporative demand. It approximates actual evapotranspiration under conditions of adequate water supply (Stephenson, 1998). The parameter AET/PET, also called the Priestley–Taylor coefficient, is commonly used as one of the main climatic controls on the vegetation distribution at continental or global scales (Prentice *et al.*, 1992; Sykes *et al.*, 1996).

First, we calculate PET and AET at the meteorological stations using the water balance model. At this stage, the estimation error for AET and PET cannot be calculated because we do not have measurements of these variables at the meteorological stations. Second, AET and PET are interpolated separately at each sampling site, using a weighted average method according to the inverse distance and after reduction at sea level (Goeury & Guiot, 1996). Third, the ratio AET/PET was calculated. The error in AET/PET induced by the interpolation method has been calculated by comparison of the interpolations at the meteorological stations with the values obtained by the water balance model. This error standard deviation is *c.* 0.04. From south to north of the studied zone, AET/PET regularly decreases from 0.45 ± 0.04 to 0.05 ± 0.04. Interpolated AET/PET are presented for each sampling site (Table 2).

Methods

Phytolith extraction, classification and counting

Phytoliths were extracted from 20 g of dry soil sieved at 2 mm, after (1) dissolution of carbonates, using HCl (3%); (2) oxidation of organic matter, using H_2O_2 (30%) heated at 90 °C until reaction subsides; (3) sieving at 60 μm; (4) removal of clays after sedimentation; (5) densimetric separation of phytoliths ($d < 2.3$) from the 2 to 60 μm fraction in a heavy liquid of $ZnBr_2$ ($d = 2.3$) (Kelly, 1990).

The recovered fraction, including opal phytoliths and diatom fragments, was mounted on microscope slides in glycerin for 3D observation and in Canada Basalm for counting. Microscopic observations are done at 600× magnification. More than 200 phytoliths with a diameter of greater than 5 μm and with taxonomic significance (classified phytoliths) were counted. Phytoliths without taxonomic significance (non-classified phytoliths) because of their original shape, or subsequent dissolution or fragmentation, were also counted. Assemblages are presented as percentages of the sum of classified phytoliths. Double counting of the same slide by a single person gave a reproducibility (SD) of ± 3.5%.

Table 1 Location, vegetation types, averaged 'observed' AET/PET (obtained by a water balance model and interpolated at the sites), phytolith indices, averaged phytolith-estimated AET/PET for samples from the Sonoran desert (Mexico), Kandara (Cameroon) and Masoko (Tanzania)

Sample sites	Number of samples	Longitude	Latitude	Vegetation types	Averaged observed AET/PET	Iph	Fs	D/P	Averaged AET/PET estimated from phytoliths
Sonora (Mexico)	7	113°20′ W	31°50′ N	Desert	0.12 ± 0.04	53.07	15.8	0.05	0.19 ± 0.04
Kandara (Cameroon)	26	13°43′ E	4°20′ N	Forest and tall grass savanna	0.94 ± 0.04	0.02	6.29	2.02	0.40 ± 0.02
Masoko (Tanzania)	10	34°45′ E	8°20′ S	Woodland	0.62 ± 0.04	8.35	15.29	0.68	0.32 ± 0.01

Table 2 Detailed counts of modern phytolith assemblages from West Africa, phytolith indices and climate data

Sample names	Latitude °N	Longitude °E	Cone-shaped	Crenate spherical	Rough spherical	Smooth spherical	Point-shaped	Fan-shaped (Fs)	Dumbbell	Cross	Saddle	Sum	Non-classified	Iph %*	Fs%**	D/P***	AET/PET	Annual rainfall (mm)
RIM 3	21.53	−13.00	0	2	4	5	36	52	18	0	6	123	143	25.00	42.28	0.04	0.05	91
RIM 8	21.03	−12.15	1	7	5	2	46	43	13	0	5	122	172	27.78	35.25	0.05	0.06	98
MAU 07	20.93	−12.20	0	2	9	11	53	56	37	1	11	180	202	22.45	31.11	0.06	0.06	99
MAU 06	20.63	−12.63	3	0	4	5	55	55	61	0	6	189	263	8.96	29.10	0.02	0.06	102
MAU 05	20.40	−13.03	1	1	1	2	44	44	26	3	5	127	262	14.71	34.65	0.01	0.06	103
MAU 04	20.23	−13.37	1	3	4	5	53	53	49	2	21	191	240	29.17	27.75	0.02	0.06	102
RIM 2	19.93	−14.08	1	3	5	6	54	62	8	0	2	141	242	20.00	43.97	0.04	0.06	101
RIM 11	16.93	−15.20	0	0	2	3	55	93	45	0	41	239	299	47.67	38.91	0.01	0.16	225
RIM 10	16.73	−15.17	0	0	6	2	36	90	22	1	16	173	349	41.03	52.02	0.04	0.17	227
R1M 1	16.68	−15.97	2	3	18	9	38	97	35	1	5	208	271	12.20	46.63	0.10	0.16	230
83-35	16.50	−14.60	2	0	4	1	67	78	5	5	27	189	128	72.97	41.27	0.02	0.16	226
S.33	16.39	−14.82	4	0	12	4	29	27	114	5	46	241	163	27.88	11.20	0.05	0.17	234
S.32	16.29	−15.35	0	1	1	4	36	37	48	5	22	154	191	29.33	24.03	0.01	0.18	256
83-30	16.17	−14.93	2	0	5	2	37	39	85	6	23	199	310	20.18	19.60	0.03	0.18	252
S.40	16.10	−13.89	0	0	15	3	47	45	74	4	60	248	196	43.48	18.15	0.07	0.22	313
S.29	16.08	−14.92	0	0	9	3	31	26	77	3	39	188	225	32.77	13.83	0.05	0.19	272
82-47	16.00	−14.95	3	3	12	3	37	46	148	7	31	290	303	23.17	16.87	0.02	0.23	348
82-46	16.00	−15.95	5	0	5	1	32	42	119	7	38	249	136	16.67	15.86	0.04	0.21	289
S.27	15.92	−14.86	2	0	1	0	42	18	104	9	53	229	162	31.93	7.86	0.00	0.22	302
S.44	15.83	−13.47	0	0	3	2	40	42	94	10	30	221	221	22.39	19.00	0.01	0.26	370
S.24	15.69	−14.99	0	0	1	1	17	13	129	1	34	196	225	20.73	6.63	0.01	0.26	368
83-46	15.43	−13.35	1	1	6	2	22	17	125	22	67	263	162	31.31	6.46	0.02	0.27	386
83-20	15.42	−15.12	5	0	8	2	26	16	95	14	77	243	212	41.40	6.58	0.04	0.29	397
83-15	15.33	−15.47	0	1	4	2	27	22	28	8	11	103	164	23.40	21.36	0.04	0.28	400
S.54	15.31	−12.99	0	0	2	3	52	32	96	3	24	212	209	19.51	15.09	0.01	0.29	447
83-48	15.28	−13.45	1	1	4	1	42	58	82	14	47	250	214	32.87	23.20	0.02	0.28	421
S.12	15.21	−15.17	0	3	16	12	46	25	72	2	19	195	305	20.43	12.82	0.10	0.28	397
S.58	15.06	−12.81	0	0	4	3	44	19	96	8	60	234	194	36.59	8.12	0.02	0.32	523
83-8	14.90	−15.85	2	9	15	4	28	47	95	10	53	263	168	33.54	17.87	0.06	0.30	482
83-62	14.85	−12.33	1	2	2	3	62	27	57	18	48	220	183	39.02	12.27	0.01	0.33	528
S.7	14.79	−15.99	0	1	11	15	53	50	66	0	3	199	227	435	25.13	0.06	0.30	507
83-65	14.75	−12.25	1	0	5	1	12	6	139	14	49	227	275	24.26	2.64	0.02	0.33	539
S.5	14.72	−16.16	0	0	19	4	29	57	51	0	13	173	167	20.31	32.95	0.13	0.30	505
83-4	14.70	−16.50	1	9	33	3	58	49	77	12	16	258	152	15.24	18.99	0.16	0.30	509
82-77	14.63	−16.32	1	1	12	3	30	41	104	16	29	237	88	19.46	17.30	0.05	0.30	505
82-79	14.17	−16.10	1	1	1	3	28	14	122	13	30	213	531	18.18	6.57	0.00	0.32	572
83-75	14.12	−12.67	0	0	11	1	29	25	131	22	22	241	213	12.57	10.37	0.05	0.36	664
82-78	14.08	−16.05	0	2	20	5	23	12	191	13	22	288	334	9.73	4.17	0.08	0.32	572
83-70	14.05	−12.27	0	0	1	0	21	5	180	17	13	237	126	6.19	2.11	0.00	0.36	667

Table 2 *continued*

Sample names	Latitude °N	Longitude °E	Cone-shaped	Crenate spherical	Rough spherical	Smooth spherical	Point-shaped	Fan-shaped (Fs)	Dumbbell	Cross	Saddle	Sum	Non-classified	Iph %*	Fs%**	D/P***	AET/PET	Annual rainfall (mm)
83-83	13.97	−13.32	4	0	1	0	14	6	178	21	14	238	176	6.57	2.52	0.00	0.38	739
S.84	13.93	−13.41	0	0	3	0	26	10	148	24	18	229	279	9.47	4.37	0.01	0.38	755
83-68	13.88	−12.25	2	1	10	2	39	13	152	15	12	246	213	6.70	5.28	0.04	0.37	716
S.118	13.63	−13.74	1	0	7	1	2	24	128	7	11	181	252	7.53	13.26	0.04	0.39	779
S.88	13.60	−13.56	0	1	5	4	19	17	155	5	29	235	207	15.34	7.23	0.02	0.39	780
S.91	13.59	−13.40	0	19	70	12	32	23	82	16	4	258	255	3.92	8.91	0.45	0.39	781
83-120	13.48	−13.83	0	1	14	6	24	12	176	10	11	254	292	5.58	4.72	0.06	0.39	812
83-122	13.35	−14.93	2	0	4	2	19	17	178	11	21	254	366	10.00	6.69	0.02	0.38	825
S.122	13.35	−13.94	1	0	0	0	17	20	93	10	13	154	341	11.21	12.99	0.00	0.40	863
S.93	13.31	−13.23	3	6	6	2	23	13	154	13	11	231	154	6.18	5.63	0.03	0.39	812
83-98	13.08	−12.83	0	1	6	1	5	2	136	16	S	175	279	5.00	1.14	0.04	0.41	909
83-127	13.07	−14.08	0	2	81	10	49	32	75	4	5	258	163	5.95	12.40	0.49	0.40	887
S.128	13.03	−14.10	0	1	7	18	45	38	118	0	9	236	288	7.09	16.10	0.03	0.40	886
83-100	13.03	−12.63	1	0	14	4	18	10	172	11	13	243	117	6.63	4.12	0.06	0.42	982
S.130	12.92	−14.17	0	0	5	2	31	29	91	10	13	181	285	11.40	16.02	0.03	0.40	882
83-103	12.92	−12.43	3	1	9	2	17	13	145	19	9	218	349	5.20	5.96	0.04	0.44	1087
S.138	12.88	−14.86	1	0	11	6	42	42	75	4	11	192	213	12.22	21.88	0.06	0.39	896
S.136	12.85	−14.74	0	0	10	2	42	57	39	3	13	166	238	23.64	34.34	0.06	0.39	890
83-116	12.67	−12.18	2	1	1	0	8	2	148	8	4	174	432	2.50	1.15	0.01	0.46	1183
S.155	12.55	−16.30	0	56	144	8	2	10	10	1	6	237	96	35.29	4.22	4.97	0.40	1283
83-151	12.48	−16.58	0	54	158	19	8	5	8	2	0	254	119	0.00	1.97	6.87	0.40	1267
83-115	12.40	−12.30	1	0	7	2	10	7	214	6	12	259	206	5.17	2.70	0.03	0.45	1175

Phytolith indices are expressed as follow:

*Iph = Chloridoideae phytoliths (saddle type) / (Chloridoideae + Panicoideae phytoliths (saddle + cross + dumbbell types)).

**Fs = % fan-shaped types.

***D/P = Ligneous dicotyledon phytoliths (rough spherical types) / Poaceae phytoliths (saddle + cross + dumbbell + point + fan-shaped types).

AET/PET = actual annual evapotranspiration / annual potential evapotranspiration, interpolated for the sampling sites (error = ± 0.04).

Phytoliths are classified according to the classification of Twiss *et al.* (1969) and Twiss (1992), augmented by Mulholland (1989), Fredlund & Tieszen (1994), Kondo *et al.* (1994), Alexandre *et al.* (1997) and Barboni *et al.* (1999). Ten phytolith types were identified. They are illustrated in Fig. 2.

Four phytolith types are produced by non-grass taxa. The cone-shape type (1) is attributed to the Cyperaceae (sedge) (Le Cohu, 1973; Ollendorf, 1987; Kondo *et al.*, 1994; Wallis, 2003). The crenate spherical phytolith type (2) is produced by Palmae (Kondo *et al.*, 1994; Runge, 1999; Runge & Fimbel, 1999; Vrydaghs & Doutrelepont, 2000). The rough spherical phytolith type (3) is produced by the wood of tropical trees and shrubs (ligneous dicotyledon) (Scurfield *et al.*, 1974; Kondo *et al.*, 1994; Alexandre *et al.*, 1997). The smooth spherical type (4) appears to have several origins. According to Kondo *et al.* (1994), this type is produced in the epidermis of leaves and in the ray or parenchyma cells of dicot twigs and wood. They have been recovered in small proportions from several tropical herbaceous monocots and in greater quantities from a small number of tropical arboreal dicot leaves and seeds (Piperno, 1988). A recent investigation of tropical grasses showed that the smooth spherical type is also produced in significant amounts by grass roots (Alexandre *et al.*, 2000).

The following types are produced by grasses: the point-shaped type (5) originates from micro-hair or prickles of all grass epidermis (Palmer *et al.*, 1985; Kaplan *et al.*, 1992). The fan-shaped phytolith type (6) (Twiss *et al.*, 1969; Kondo *et al.*, 1994) are produced in bulliform cells, also called motor-cells, of all grass epidermis. Although bulliform cells may also occur in sedges, no silicified bulliform cells have been observed in sedges up to now. Silicified short cells from the grass epidermis, the dumbbell (7) and cross (8) types occur predominantly in the Panicoideae subfamily (Twiss *et al.*, 1969; Mulholland, 1989; Fredlund & Tieszen, 1994; Kondo *et al.*, 1994), which includes predominantly tall C_4 grasses adapted to warm climate and high available soil moisture (Teeri & Stowe, 1976; Tieszen *et al.*, 1979; Cabido *et al.*, 1997; Scott, 2002). The saddle type (9) is produced in high proportions by the Chloridoideae subfamily (Twiss *et al.*, 1969; Mulholland, 1989; Fredlund & Tieszen, 1994; Kondo *et al.*, 1994), a group of short C_4 grasses adapted to warm and dry climate or low available soil moisture (Tieszen *et al.*, 1979; Livingstone & Clayton, 1980). The elongate type (10) originates from the silicified long cells of the epidermis of all grasses. Because it may be confused with weathered diatoms or sponge spicules, this type was included in the non-classified group.

Calculation of phytolith indices

Phytolith data will be discussed through three phytolith indices, as described below. Two of them are commonly in use in phytolith studies: the tree cover density index (D/P) and the humidity-aridity index (Iph).

Tree cover density index. The D/P index is the ratio of the rough spherical phytoliths, produced by tropical woody dicotyledons, to the sum of Poaceae phytoliths (dumbbell, cross, saddle, point-shaped and fan-shaped types). It was first used by Alexandre *et al.* (1997) in West and Central Africa in order to estimate the tree cover density. In modern samples, a D/P value of 7 was found in a semi-evergreen forest in Congo, whereas values lower than 0.2 characterize savannas with various tree cover densities in Senegal. However, Alexandre *et al.* (1997) did not distinguish elongated phytolith types from point-shaped and fan-shaped types. So, the D/P index used here, which excludes the elongated types in the sum of Poaceae phytoliths, should be higher. Barboni *et al.* (1999) calculated a D/P ratio of 0.1 for a shrub steppe and of 0.7 for the margin of a riparian forest on the west side of the Middle Awash valley (Ethiopia). The error assigned to this index is 7% (SD on rough spherical type plus maximum SD on Poaceae phytolith types).

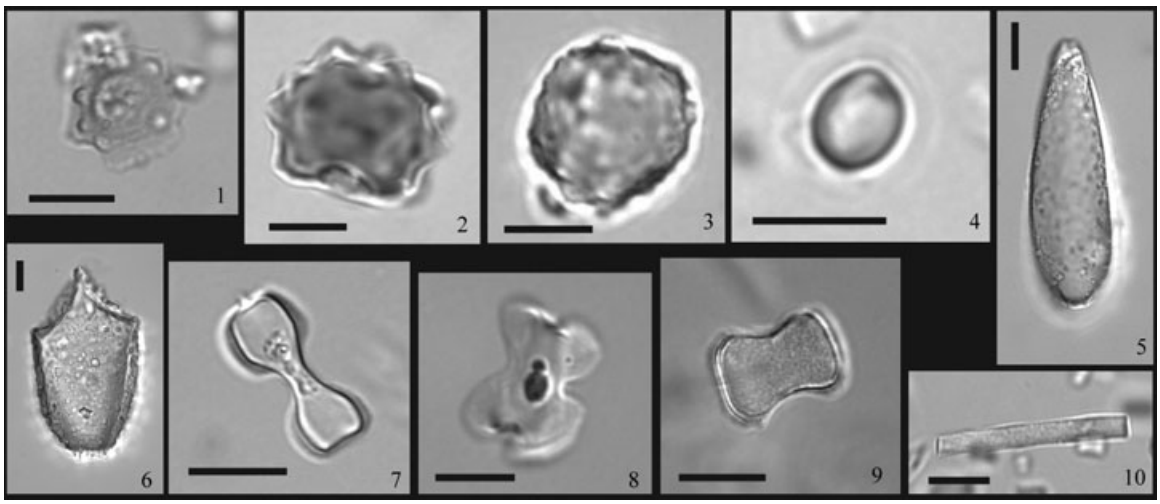

Figure 2 Microphotographs of representatives of the 10 types of identified phytoliths; Scale bar = 10 μm: (1) cone shaped type; (2) crenate spherical type; (3) rough spherical type; (4) smooth spherical type; (5) point-shaped; (6) fan-shaped type (also Fs); (7) dumbbell type; (8) cross type; (9) saddle type, (10) elongate type.

Humidity-aridity index. The Iph index is the ratio of Chloridoideae type (saddle type) to the sum of Chloridoideae and Panicoideae types (saddle, cross and dumbbell types). This index was first defined by Diester-Haass *et al.* (1973) from assemblages from marine sediments off West Africa to identify humid-arid transitions in West Africa during Pleistocene and Holocene. It was later used for vegetation reconstructions from continental sediments, soils and buried soils from African, Brazilian and Mediterranean sites (Alexandre *et al.*, 1997; Barboni *et al.*, 1999; Delhon *et al.*, 2003). High Iph values (> 20–40%) record grasslands dominated by Chloridoideae, i.e. xerophytic short grass savannas, and hence the prevalence of warm and dry climatic conditions. Conversely, low Iph values (< 20–40%) indicate associations in which Panicoideae, i.e. mesophytic C_4 grasses dominate, suggesting warm and humid climate and/or high available soil moisture. However, local association of perennial Panicoideae grasses with annual Chloridoideae may occur in Saharan desert zones (Le Houérou, 1993a). Such vegetation will induce low Iph (< 20–40%) connected to local conditions, despite the regional dryness. The geographical scale recorded by phytolith assemblages will be discussed later. The error assigned to this index is ± 7% (SD on saddle type plus max SD of saddle, cross or dumbbell types).

Water-stress index. We define a third phytolith index, Fs, as the percentage of the fan-shaped phytolith type in relation to the sum of grass phytoliths minus the elongate phytolith type. Hypotheses on its environmental significance are discussed later, considering statistical relationships between phytolith indices and AET/PET data. The error assigned to this index is ± 3.5% (SD on fan-shaped type).

Statistical analysis for estimating AET/PET from phytolith and pollen data

The relationship between phytolith indices and AET/PET is based on the samples from West Africa. Bootstrapped regression methods were used to evaluate the strength of the data analyses, and were performed using the software PPPbase (Goeury & Guiot, 1996). The bootstrapping regression method (Efron, 1979; Guiot, 1990) is a technique to estimate, by simulations, statistics for unknown population distributions. Original observations are re-sampled in a suitable way to construct pseudo data sets on which the estimates are performed. Each pseudo data set has the same size as the raw data set and is composed by random extraction with replacement. The suitable statistics (e.g. means, SDs, correlations, regression coefficients) are calculated for each pseudo data set and are averaged to provide the bootstrap estimate. Variability of the calculated quantity among the various pseudo data sets provides us with the required confidence intervals. Only a portion of the samples is used in each pseudo data set. The remaining data are used for independent verification.

The AET/PET values estimated from phytoliths are compared with the values estimated from pollen. Pollen taxa are assigned to plant functional types (PFTs), which are, for that purpose, broad classes of plants defined by stature, leaf form, phenology and bioclimatic factors. For each modern spectrum, a score is calculated for each PFT, given as the sum of the square root of the percentage of taxa belonging to the PFT. This method, called the 'biomization method' was developed by Jolly *et al.* (1998) using African pollen data and was slightly modified by Peyron *et al.* (2000). Using an artificial neural network technique, these PFT scores are then calibrated in terms of AET/PET (Peyron *et al.*, 2000) using the PPPbase (Goeury & Guiot, 1996).

In order to check the reliability of the relationships for other geographic areas, while remaining at the boundary of the climatic conditions chosen for the calibration, three sets of modern phytolith assemblages from Mexico, Cameroon and Tanzania are also analysed (Table 1). Error is calculated by orthogonal bootstrap regression.

RESULTS

Phytolith assemblages

Phytolith assemblages are presented in Fig. 3 and Table 2. In all assemblages, the Cyperaceae phytolith (cone-shape type) is weakly represented (less than 2 ± 0.07%), as expected because of its sensitivity to dissolution and fragmentation in litter and soil (Alexandre *et al.*, 1997). The Palmae phytolith (crenate type) accounts for less than 7 ± 0.25% in most of the samples but reaches values higher than 20 ± 0.7% in samples from forests of the Guinean zone (S.155 and 83–151). The rough spherical type produced by tropical woody dicotyledons presents an average value of 20 ± 0.7% in the Guinean zone, 6 ± 0.2% in tall-grass savannas of the Sudanian zone, 3 ± 0.1% in short-grass savannas of the Sahelian zone and 3 ± 0.1% in the Saharan zone. The smooth spherical type ranges from 0% to 8 ± 0.28% and does not show any pattern specific to the vegetation.

Within the group of phytoliths diagnostic of Poaceae, the point-shaped phytolith type accounts for 1 to 38 ± 1.33%. The percentage of this phytolith type increases from the Guinean to the Saharan zone. The dumbbell type reaches very high values in the Sudanian tall grass savanna zone (from 29 ± 1% to 85 ± 2.97% with an average of 58 ± 2.03%) compared with the Sahelian zone (from 2 ± 0.07% to 65 ± 2.28% with an average of 37 ± 1.3%). The cross phytolith type also reaches its maximum abundance (from 0 to 10 ± 0.35%) in the Sudanian zone. The saddle type accounts for 0 to 32 ± 1.12%, and is more abundant in the Sahelian short grass savanna zone (from 2 ± 0.07% to 32 ± 1.16% with an average of 17 ± 0.6%) than in the Sudanian zone (from 1 ± 0.04% to 14 ± 0.49% with an average of 7 ± 0.25%).

Phytolith indices

Tree cover density index

The D/P ratio is always lower than 1 except in rain forests (S.155 and 83–151) where it reaches 5 and 7.

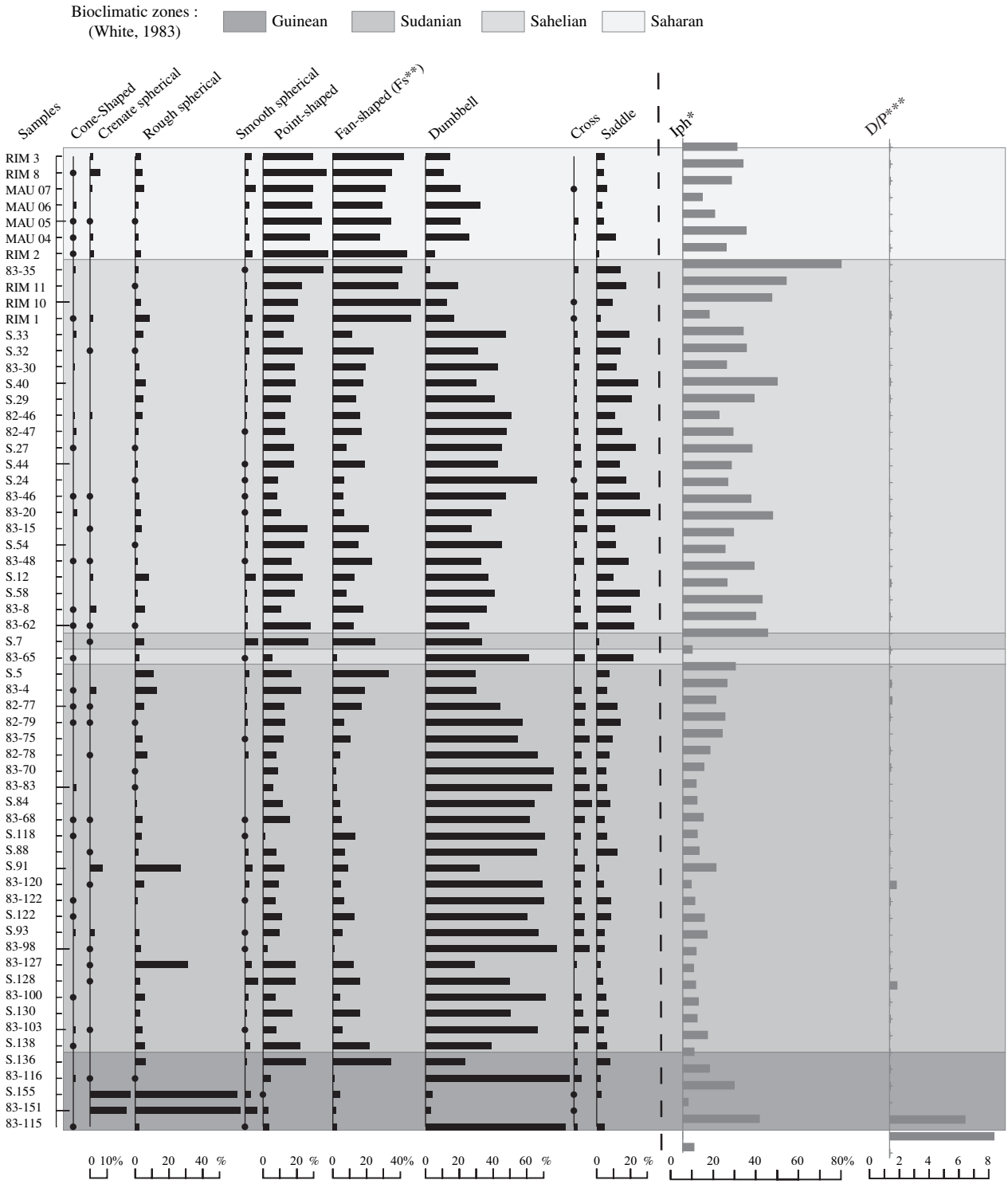

Figure 3 Phytolith assemblages: abundances of phytolith types are expressed as percentage of the classified phytolith sum. Abundances lower than 1% are identified by a dot. Phytolith indices are expressed as follow: *Iph = Chloridoideae phytoliths (saddle type)/[Chloridoideae + Panicoideae phytoliths (saddle + cross + dumbbell types)]. **Fs = % fan-shaped types. ***D/P = Ligneous woody dicotyledon phytoliths (rough spherical types)/Poaceae phytoliths (saddle + cross + dumbbell + point + fan-shaped types).

Humidity-aridity index

An increasing trend of Iph index from the Guinean to the Sudanian zone clearly appears. Most of the Sudanian and Guinean samples (23 vs. 25 samples) present an Iph index lower than 20 ± 1.4%, except two samples taken from the rain forest (S.155, Iph = 35 ± 2.45%) and on the Casamance

grassy riverside (S.136 = 24 ± 1.68%). Most of the Sahelian samples (21/24) are characterized by an Iph index higher than 20 ± 1.4%. Sample S.54, with an Iph of 19.5 ± 1.37%, is not far from the previous value. Two samples (RIM 1 and 82-47) present values of 12.2 ± 0.85% and 16.7 ± 1.17%, respectively, clearly lower than 20 ± 1.4%. The first one (RIM 1) is located in a tree savanna (*Acacia* and *Balanites*) while the second one (82-47) is taken along the shore of Lake Guiers. Saharan samples show variable Iph indices ranging from 9 ± 0.63% to 29 ± 2.03%.

Water-stress index

The Fs index generally increases from the southern to the northern samples (0–52 ± 1.82%). In the Guinean, Sudanian and Sahelian zones, Fs values are less than 25 ± 0.88% except for samples S.5 and S.136 (33 ± 1.16 and 34 ± 1.19%). The four northern Sahelian samples present very high Fs values (39 ± 1.37–52 ± 1.82%), as do samples from the Saharan zone (31 ± 1.09–44 ± 1.54%).

To summarize, the Iph boundary of 20 ± 1.4% differentiates tall from short grass savanna associations in West Africa. An increasing trend of Fs with AET/PET clearly appears.

Statistical relationships between AET/PET and phytolith indices

Figures 4 and 5 show that the Fs and Iph indices are negatively correlated with AET/PET from the Guinean to the Sahelian zone. Calibration of the relationship between AET/PET and these two indices is made using the following bootstrapped quadratic regression:

$$\text{AET/PET}\ (\%) = a_0\text{Fs} + a_1\text{Iph} + a_2(\text{Iph} - 20)^2$$

where the coefficients $a_0 = -0.605 \pm 0.075$, $a_1 = -0.387 \pm 0.087$ and $a_2 = 0.272 \pm 0.068$ are the regression coefficients. The two regressors Fs and Iph are the previously defined phytolith indices. The quadratic term $(\text{Iph} - 20)^2$ is introduced in order to take into account the decreasing Iph index in the Saharan zone. The value of 20 is the Iph average calculated from our data set.

The multiple correlation coefficient between estimated and observed values of AET/PET is 0.80 ± 0.04 (SD). The (independent) verification correlation is 0.71 ± 0.14 (SD), which is highly significant. Estimated AET/PET vs. observed AET/PET and summary statistics are presented in Fig. 6.

The correlation coefficient ($R = 0.80$) with a SD of 0.04 is fairly significant ($P < 0.0001$). However over- or underestimations of AET/PET are significant (> 0.1) for nine sites.

AET/PET is overestimated by 0.13–0.19 for four Saharan samples. This is due to their low Iph index, imperfectly simulated by the third regressor $(\text{Iph} - 20)^2$, and certainly to their proximity to the four samples from the northern Sahelian zone that present much higher values of Fs than samples from the desert zone. However, the regression is better when using the third regressor $(\text{Iph} - 20)^2$ than when using only two regressors ($R = 0.76 \pm 0.04$). An alternative approach could be to remove the Saharan samples to maintain the linearity of the relationship but this would make it applicable only in non-desert environments. When we do this, the regression is also worse ($R = 0.76 \pm 0.04$). AET/PET is also overestimated by +0.11 for the Sahelian sample S.33, due to a low Fs. Underestimation of AET/PET by −0.12 for RIM 10 (northern Sahelian zone), −0.12 for S.5 (Sudanian zone), −0.23 for S.136 and −0.12 for S.138 (Guinean zone) is linked to their high Fs indices (34.3 ± 1.2% and 21.8 ± 0.76%) instead of elevated values of observed AET/PET (0.39). Local water stress or high transpiration, leading to the production of high amounts of the fan-shaped phytolith type, may explain such high Fs values (see Discussion).

In order to check the reliability of the relationships for other geographic areas, while remaining at the boundary of the climatic conditions chosen for the calibration, three sets of modern phytolith assemblages are processed (Table 1). Samples from the Sonoran desert (Mexico) present low observed AET/PET (0.12 ± 0.0.4), while sample sites from Cameroon and Tanzania are much more humid (AET/PET is respectively 0.94 ± 0.04 and 0.62 ± 0.04) than the wettest site of our

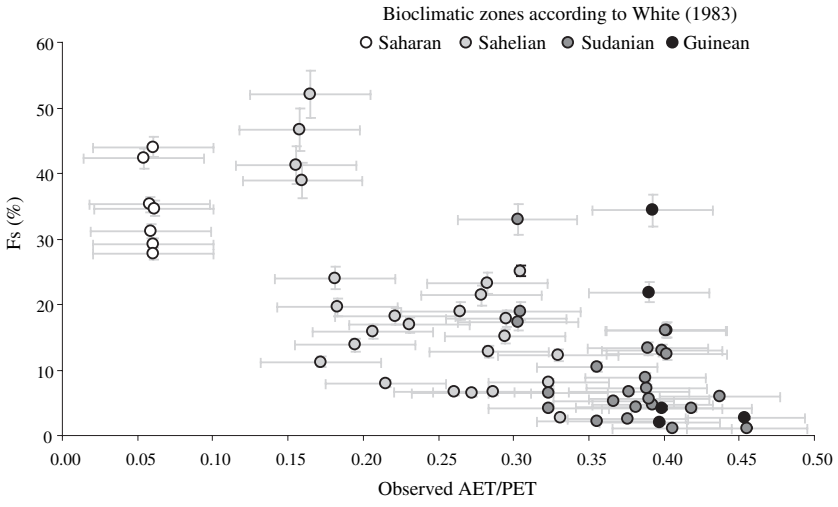

Figure 4 Fs index [% fan-shaped types (classified phytoliths − elongate phytolith types)] vs. AET/PET for the West African samples. Error from the interpolation method for observed AET/PET has been estimated at 0.04. The error assigned to the Fs index is 3.5% (SD on the fan-shaped type).

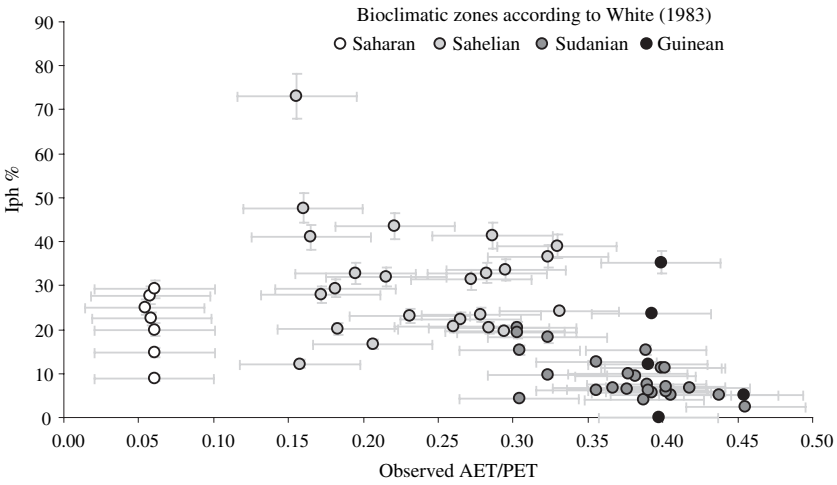

Figure 5 Iph index (*Chloridoideae* phytoliths (saddle type)/[*Chloridoideae* + *Panicoideae* phytoliths (saddle + cross + dumbbell types)] vs. AET/PET for the West African samples. The error (SD) from the interpolation method for observed AET/PET has been estimated at 0.04. The error (SD) assigned to the Iph index is 7% (SD on the saddle type plus maximum SD of the saddle, cross or dumbbell types).

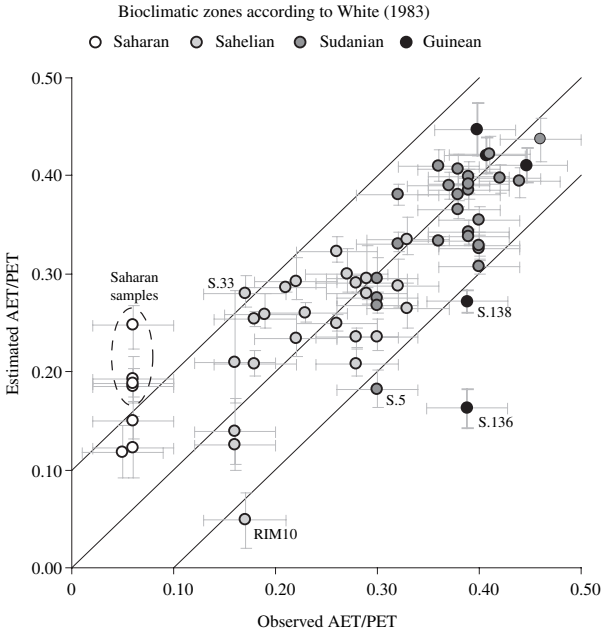

AET/PET (%) =	
42.497 (constant)	
-0.538 Fs	
-0.326 Iph	
+0.008 (Iph-20)2	
Summary statistics	
Number of observations	61
Number of regressors	3
Multiple correlation coefficient (R)	0.796
Standard deviation (s.d.)	0.039
Verification correlation (R)	0.708
Standard deviation (s.d.)	0.142

Figure 6 AET/PET estimated from phytolith indices vs. 'observed' AET/PET (obtained by a water balance model and interpolated at the sites), for the West African samples. Error (SD) from the interpolation method for observed AET/PET has been estimated at 0.04. Error (SD) of estimated AET/PET is calculated by orthogonal bootstrap regression.

calibration set (0.46 ± 0.04). The results show that AET/PET is over-estimated for the Sonoran desert samples by 0.07, which is at the limit of the confidence interval. This over-estimation is due to two Saharan samples, used for the calibration set, showing a low Iph, relative to the local occurrence of perennial Panicoideae grass (Le Houérou, 1993b), and a low Fs (10 ± 0.35%). It may also be due to the difficulty in calculating such a parameter from meteorological observations in desertic environments. AET/PET calculated for Cameroon and Tanzania are underestimated by 0.54 and 0.3, respectively, which is much more significant. The reason is that the regression equations have been established from West African samples, where low values of Fs and Iph occur, with values of AET/PET between 0.40 and 0.45. It is then impossible for the regression to produce values of AET/PET higher than 0.45 with null values of Fs and Iph.

Finally, these results show that AET/PET is estimated from phytolith indices with good accuracy for the Sahelian, Sudanian zones and Guinean zones. It is over-estimated by 0.13–0.19 for the Saharan zone. The phytolith proxy presented here can be applied to other inter-tropical areas for estimating AET/PET ranging from 0.1 ± 0.04 to 0.45 ± 0.04.

Comparison between phytolith and pollen-derived estimations of AET/PET

Figure 7 gathers observed and estimated AET/PET from phytolith data presented in this study and pollen data presented in Peyron (1999), covering the same sampling zones but different sampling sites. Differences between observed and estimated AET/PET by pollen are usually lower than 0.1. Over- or under-estimations of AET/PET are significant (> 0.1) for only five of 74 sites. Figure 7 shows that pollen estimation is slightly better than phytolith estimation, with correlation coefficients and standard deviation of 0.84 ± 0.04 (bootstrap verification set: $r = 0.76 \pm 0.08$) and 0.80 ± 0.04, respectively. In the Sudanian and Guinean zones, AET/PET is estimated as well by phytoliths as it is by pollen (mean error = +0.03). AET/PET values of Sahelian samples are very well estimated by phytoliths (mean error = + 0.01) and by pollen (mean error = −0.02). In the Saharan zone AET/PET is overestimated by pollen (mean error = −0.02) and is overestimated by phytoliths (mean error = + 0.11).

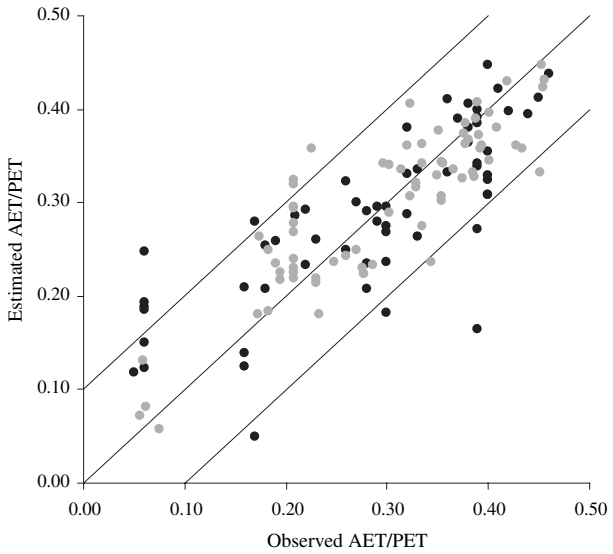

Summary statistics

Number of observations : - Phytoliths	61	●
- Pollens	62	●
Correlation coefficient (R), standard deviation (s.d.)		
- Phytoliths	0.80 ± 0.04	
- Pollen	0.84 ± 0.04	

Figure 7 Observed and estimated AET/PET from phytolith (black points) and pollen data (grey points) for the West African samples. Error from the interpolation method for observed AET/PET has been estimated at 0.04. Error of phytolith and pollen estimated AET/PET is calculated by orthogonal bootstrap regression.

Finally, pollen and phytolith data are complementary for estimating AET/PET in the Guinean and Sudanian zones. Phytoliths provide improved estimation for the Sahelian zone. However, AET/PET of Saharan samples appear less well estimated by the phytoliths, although these discrepancies between observed and estimated values is related to the difficulty taking into account the local occurrence of perennial Panicoideae grasses as occur in the Saharan zone.

DISCUSSION

Spatial scale recorded by the phytolith assemblages

The four bioclimatic zones are clearly distinguished through AET/PET estimation made from phytolith analysis, although some discrepancies between observed and estimated data occur due to local vegetation features. Phytolith assemblages from these areas are sensitive to the local vegetation but are also connected to zonal vegetation dominance. Indeed, in tropical areas and especially in arid areas, the extent of open vegetation, the high frequencies of fires and the strength of the trade winds would favour aeolian transportation of phytoliths. Aeolian transportation of Saharan dust in quantities and over long distances is well documented (Ruddiman, 1997; Grousset *et al.*, 1998; Ratmeyer *et al.*, 1999a,b; Chiapello & Moulin, 2002). Phytolith studies of sediments from the Atlantic Ocean, off the west and northwest African coast, show that phytoliths from West Africa are also subject to long distance transportation (Diester-Haass *et al.*, 1973; Flores *et al.*, 2000; Abrantes, 2003). The two major continental wind systems that are likely to transport West African particles are the low altitude north-easterly trade winds in winter, and the mid altitude African Easterly Jet in summer (Huang *et al.*, 2000; Zhao *et al.*, 2000; Abrantes, 2003). At the latitude of the Saharan zone, north-easterly trade winds prevail as the transport agent (Huang *et al.*, 2000), which should not affect the sensitivity of phytolith assemblages to zonal vegetation. At the latitudes of the Sahelian, Sudanian and Guinean zones, the north-easterly trade winds and the African Easterly Jet alternate (Ratmeyer *et al.*, 1999b; Huang *et al.*, 2000). While the African Easterly Jet is parallel to the vegetation zones, the trade winds should transport phytoliths southward, reducing differences between Sahelian, Sudanian and Guinean phytolith assemblages. This aeolian transport should also affect pollen records. However, wind transportation does not prevent a clear distinction between Saharan, Sahelian, Sudanian and Guinean phytolith assemblages.

Significance of the Iph index in term of C_4-grassland physiognomy and water stress (AET/PET)

The Iph index is considered in this study to reflect the dominance of short C_4 grasses (mainly Chloridoideae) vs. tall-C_4 grasses (mainly Panicoideae) in a given vegetation zone. Because Chloridoideae species tolerate high temperature extremes and aridity better than other grasses (Jacobs, 1987), the Iph index is also dependent on the humidity–aridity balance. Wyk (1979) established through field and bibliographic study that the dominant Chloridoideae genera of Africa (*Chloris* and *Eragrostis*) are characteristic of dry tall grass savannas from Sudanian areas with less than 700 mm year^{-1} of rainfall and of Sahelian short grass savannas. However, the relationships between high Iph index, short C_4-grass dominance and aridity may exhibit some exceptions for the following reasons. (1) Some Panicoideae are annual short grasses adapted to local humid areas in arid zones. An example is *Panicum turgidum*, a Panicoideae perennial short-grass (Hutchinson & Dalziel, 1968–72; Le Houerou, 1988) found in the Sahara, which produces assemblages with high Iph values instead of reflecting the regional desert conditions. This example explains the several discrepancies between observed and estimated AET/PET using phytolith analysis, as pointed out earlier. (2) Grass communities may include large amounts of grasses from the Arundinoideae subfamily which produces both phytolith types categorized as 'Panicoideae' (e.g. *Aristida*, *Stipa*) and 'Chloridoideae' (e.g. Phragmites) types and may influence the Iph index in one way or another. For example, Arundinoideae grasses in the Sahelian zone are mainly represented by *Aristida* (Tronchain, 1940), which may lower the Iph index. However, Arundinoideae grasses are never dominant in the West African grasslands (Tronchain, 1940; Wyk, 1979), which limits their effect on the Iph index.

This study confirms that the Iph index is a good indicator of short and tall grass savannas in West Africa. As tall and short grass dominance is also related to AET/PET (Parton *et al.*, 1994; Stephenson, 1998) the Iph index may also be related to AET/PET ranges: Iph values higher than 20 ± 1.4% characterize 22 of the 24 short grass savannas growing under AET/PET values ranging from 0.15 ± 0.04 to 0.30–0.35 ± 0.04, while Iph values lower than 20 ± 1.4% characterize 23 of the 25 tall grass savannas growing under AET/PET values ranging from 0.30–0.35 ± 0.04 to 0.45 ± 0.04 and three of the seven desert C_4 grasslands growing under AET/PET values of 0.05 ± 0.04. This result requires us to reassess the Iph boundary of 30% previously suggested by Alexandre *et al.* (1997) after studying five samples from our set of 62 samples. The Iph boundary of 20% ± 1.4 is lower than the Iph boundary of *c.* 40% calculated from Kurmann's (1985) and Fredlund & Tieszen's (1997) data, which discriminates tall grass prairies from short grass prairies recorded by Pleistocene, Holocene and modern phytolith assemblages in North America. Disagreement between African and North American Iph boundaries may result from different proportions of Chloridoideae, Arundinoideae and Panicoideae grasses in North American and African short and tall grass savannas. This observation suggests that another calibration of the relationships between Iph, grassland physiognomy and AET/PET must be done specifically for the North American grasslands.

Significance of the Fs index in term of water stress (AET/PET)

Bulliform cells are part of the epidermis of grasses and other monocots such as sedges (Andrejko & Cohen, 1984). They differ from other epidermal cell in being larger and more inflated (Ellis, 1976). This type of cell occurs most commonly, but not exclusively, at the basis of adaxial furrows (Shields, 1951). The outer epidermal walls of these cells have the ability to contract in width when the leaf is dehydrated, which promotes the grass leaf-rolling response to moisture loss (O'Toole & Cruz, 1980; Hsiao *et al.*, 1984; Moulia, 1994; Hernandez *et al.*, 1999). Decreasing turgor of the bulliform cells occurs when the leaf transpires before rolling. O'Toole & Cruz (1980) also showed that the degree of leaf rolling in rice is linearly related to leaf water potential, depending on water deficit length. Thus, two factors control the leaf rolling: high transpiration and water stress.

The process involved in silicification of bulliform cells is not well documented. Parry & Smithson (1958) suggested, based on microscopy, that in developing leaves deposits of silica occur first in normal epidermal cells, and that bulliform cells accumulate silica in a later stage. According to the same authors, silica depositions in bulliform cells may completely upset their hygroscopic and water storage functions and might be an initial cause of the desiccation of the leaf. Sangster & Parry (1968) studied the formation of silicified bulliform cells in three cultivated grass species. These authors showed (by counting under the microscope the number of silicified bulliform cells per leaf area) that formation of silicified bulliform cells occur preferentially when species normally grown under dry conditions are cultivated under wet conditions. Andrejko & Cohen (1984) also suggested that the siliceous filling of bulliform cells is greatest in plants where transpiration is highest and where the root system has been submerged. According to these data, the hypothesis proposed here is that leaf rolling due to an increase of transpiration and/or an increase in duration of water stress would lead to silica saturation and precipitation. The more plants transpire and/or suffer water stress, the more silicified bulliform cells (Fs) they would produce. Our results confirm this hypothesis. Indeed, the proportion of silicified bulliform cells in phytolith assemblages (Fs) increases when regional AET/PET decreases. Local wet areas in dry zones may also induce high transpiration rates and high production of silicified bulliform cells, as suggested previously from our data.

A phytolith proxy of AET/PET: the application domain

The relationship between Iph and Fs phytolith indices and AET/PET proposed in this study applies to C_4-grassland areas where AET/PET ranges from 0 to 0.45 ± 0.04, and where rainfall and evapotranspiration are the main environmental controls on vegetation distribution. Such C_4 grasslands are common in inter-tropical areas (e.g. West Africa, South America, India and Australia) and were even more widespread during the last glacial period.

However, the proxy presented here should be used with caution when applied to phytolith assemblages with the following features:

(1) When the Chloridoideae phytolith (the saddle type) is absent from the assemblage, and when the Iph index reaches 0, the relationship presented here will underestimate AET/PET.

(2) When tropical woody dicotyledon phytoliths (the rough spherical type) show a higher abundance, another relationship should be sought, using the D/P phytolith index (tropical woody dicotyledon phytoliths vs. Poaceae phytoliths) as a fourth regressor.

(3) When C_3-grass phytoliths [the circular, rectangle or crenate types, according to Twiss *et al.* (1969); Mulholland (1989) and Fredlund & Tieszen (1994)] are also well represented, another relationship should again be calculated, that includes the Ic index (C_3-grass phytoliths vs. C_3- plus C_4-grass phytoliths) as a regressor.

In summary, the present proxy will be very useful for reconstructing past values of AET/PET when working on phytolith assemblages that are dominated by Panicoideae and Chloridoideae C_4-grass phytoliths, that are devoid of Pooideae C_3-grasses, and which occur with a few tropical woody dicotyledon phytoliths.

Archaeological evidence indicates that human activities have had a large impact on the Sahelian vegetation over the last 2000 years (Le Houérou, 1993a). Effect of overgrazing may have: (1) eliminated perennial grasses such as Panicoideae (*Andropogon*) *and* Arundinoideae (*Aristida*); and (2) replaced

mesic annual grasses of the Panicoideae subfamily by more xeromorphic grasses of the Arundinoideae and Chloridoideae subfamilies (Le Houérou, 1993a). Thus, both climate and human impact may be responsible for the current widespread distribution of Chloridoideae grasses in the Sahelian zone and for the high Iph calculated from the related modern phytolith assemblages. Past values of AET/PET may thus be underestimated when applying the present proxy to fossil phytolith assemblages with high Iph.

CONCLUSION

(1) Calibration of the relationship between phytolith indices, vegetation structure, and AET/PET, is successfully made for the West-African bio-climatic zones.
(2) Characterization of the grass cover (dominated by short Chloridoideae grasses or tall Panicoideae grasses) is accurately made through the phytolith index Iph. A boundary of $20 \pm 1.4\%$ discriminates tall grass savannas from short grass savannas.
(3) Water stress and transpiration suffered by the grass cover can be estimated through a second phytolith index Fs.
(4) These two phytolith indices can be combined to get a new proxy of the annual amount of growth-limiting drought stress for grasses, expressed by the ratio AET/PET:

$$\mathrm{AET/PET} = -0.605\mathrm{Fs} - 0.387\mathrm{Iph} + 0.272(\mathrm{Iph} - 20)^2 \; (r = 0.80 \pm 0.04)$$

The above proxy is reliable for estimating AET/PET ranging from 0.1 ± 0.04 to 0.45 ± 0.04, although very low AET/PET can be slightly over-estimated. It can be applied to fossil phytolith assemblages that are dominated by Panicoideae and Chloridoideae C_4-grass phytoliths, that are devoid of Pooideae C_3-grass phytoliths, and which occur with a few tropical ligneous woody dicotyledon phytoliths.

Finally, comparison with modern pollen data shows that phytolith and pollen proxies estimate with similar precision ($r_{\mathrm{pollen}} = 0.84 \pm 0.04$; $r_{\mathrm{phytolith}} = 0.80 \pm 0.04$) the AET/PET in the studied area. Special efforts should be made in the future to sample various types of grasslands from other geographic areas, and to analyse the related modern phytolith assemblages in term of phytolith indices.

We can suggest from these results that combining phytolith and pollen proxies of AET/PET would help to constrain this climate parameter better. As AET/PET is a bioclimatic indicator commonly used in vegetation models, such a combination would help to make model/data comparisons more efficient.

ACKNOWLEDGEMENTS

We are grateful to Anne-Marie Lézine who collected the samples in Senegal and Mauritania and made them available to us, to Martin Ortiz and Sophie Gachet who collected the samples in Mexico, and to Annie Vincens who collected the samples in Cameroon. Thanks also to Francesca Smith for language corrections. This work was supported by the French programs PNEDC (Programme National d'Etudes Dynamique du Climat, INSU-CNRS, projects ECHO and 'Calibration des indices phytolithiques pour l'intégration de la dynamique des biomes herbacés dans la modélisation des végétations passées'), ACI 'Ecologie Quantitative' (project RESOLVE), and by the 5th EU PCRDT (EVK2-CT-2002-00153: MOTIF). Pollen data are available from the African Pollen Data base (http://medias.obs-mip.fr/apd/).

REFERENCES

Abrantes, F. (2003) A 340,000 year continental climate record from tropical Africa – news from opal phytoliths from the equatorial Atlantic. *Earth and Planetary Science Letters*, **209,** 165–179.

Alexandre, A., Meunier, J.-D., Lézine, A.-M., Vincens, A. & Schwartz, D. (1997) Phytoliths indicators of grasslands dynamics during the late Holocene in intertropical Africa. *Palaeogeography, Palaeoclimatology, Palaeoecology*, **136,** 213–219.

Alexandre, A., Bouvet, M. & Meunier, J.-D. (2000) Phytolith and the biochemical cycle of silicon in a savanna ecosystem. *Third International Meeting on Phytolith Research. Man and the (palaeo)environment. The phytolith evidence* (ed. by L. Vrydaghs and A. Degraeve), pp. 1–2. Tervuren, Belgium.

Andrejko, M.J. & Cohen, A.D. (1984) Scanning electron microscopy of silicophytoliths from the Okefenokee swamp-marsh complex. *The Okefenokee swamp: its natural history, geology and geochemistry*. (ed. by A.D. Cohen, D.J. Casagrande, M.J. Andrejko and G.R. Best), pp. 468–491. Wetland Surveys, Los Alamos, NM.

Baker, R.G., Fredlund, G.G., Mandel, R.D. & Bettis, E.A. (2000) Holocene environments of the central Great Plains: multi-proxy evidence from alluvial sequences, southeastern Nebraska. *Quaternary International*, **67,** 75–88.

Barboni, D., Bonnefille, R., Alexandre, A. & Meunier, J.D. (1999) Phytoliths as palaeoenvironmental indicators, West Side Middle Awash Walley, Ethiopia. *Palaeogeography, Palaeoclimatology, Palaeoecology*, **152,** 87–100.

Blinnikov, M., Busacca, A. & Whitlock, C. (2002) Reconstruction of the late Pleistocene grassland of the Columbia basin, Washington, USA, based on phytolith records in loess. *Palaeogeography, Palaeoclimatology, Palaeoecology*, **177,** 77–101.

Cabido, M., Ateca, N., Astegiano, M.E., Anton, A.M. & Imbiv, U.-C. (1997) Distribution of C_3 and C_4 grasses along an altitudinal gradient in Central Argentina. *Journal of Biogeography*, **24,** 197–204.

Carter, J.A. (2002) Phytolith analysis and paleoenvironmental reconstruction from Lake Poukawa Core, Hawkes Bay, New Zealand. *Global and Planetary Change*, **33,** 257–267.

Chiapello, I. & Moulin, C. (2002) TOMS and METEOSAT satellite records of the variability of Saharan dust transport over the Atlantic during the last two decades (1979–1997). *Geophysical Reasearch Letters*, **29,** 1029–1032.

Claussen, M. & Esch, M. (1994) Biomes computed from simulated climatologies. *Climate Dynamics*, **9,** 235–243.

Cramer, W. (2002) Biome models. *Encyclopedia of Global Environmental Change* (ed. by T. Munn), pp. 166–171. John Wiley & Sons, Chichester.

CSA (1956) *Phytogeography*. Scientific Council for Africa South of Sahara (CCTA), Yangambi.

CSE (2000) *(Centre de Suivi Ecologique) Annuaire sur l'Environnement et les Ressources naturelles du Sénégal*. Ministère de l'Environnement, République du Sénégal. C.S.I., Dakar, pp. 268.

Delhon, C., Alexandre, A., Berger, J.-F., Thiébault, S., Brochier, J.-L. & Meunier, J.-D. (2003) Phytolith assemblages as a promising tool for reconstructing Mediterranean Holocene vegetation. *Quaternary Research*, **59,** 48–60.

Diester-Haass, L., Schrader, H.J. & Thiede, J. (1973) Sedimentological and paleoclimatological investigations of two pelagic ooze cores off Cape Barbas, North-West Africa. *Meteor Forsh-Ergebnisse*, **C16,** 19–66.

Efron, B. (1979) Bootstrap methods: another look at the jackknife. *Annals of Statistics*, **7,** 1–26.

Ellis, R.P. (1976) A procedure for standardizing comparative leaf anatomy in the Poaceae. I. The leaf-blade as viewed in transverse section. *Bothalia*, **12,** 65–109.

Flores, J.-A., Bárcena, M.A. & Sierro, F.J. (2000) Ocean-surface and wind dynamics in the Atlantic Ocean off Northwest Africa during the last 140,000 years. *Palaeogeography, Palaeoclimatology, Palaeoecology*, **161,** 459–478.

Fredlund, G. & Tieszen, L.T. (1994) Modern phytolith assemblages from the North American Great Plains. *Journal of Biogeography*, **21,** 321–335.

Fredlund, G. & Tieszen, L.T. (1997) Calibrating grass phytoliths assemblages in climatic terms: application to the late Pleistocene assemblages from Kansas and Nebraska. *Palaeogeography, Palaeoclimatology, Palaeoecology*, **136,** 199–211.

Goeury, C. & Guiot, J. (1996) PPPbase software for statistical analysis of paleoecological and palaeoclimatical data. *Dendrochronologia*, **14,** 295–300.

Grousset, F.E., Parra, M., Bory, A., Martinez, P., Bertrand, P., Shimmield, G. & Ellam, R.M. (1998) Saharan wind regimes traced by the Sr-Nd isotopic composition of subtropical Atlantic sediments: Last Glacial Maximum vs today. *Quaternary Science Reviews*, **17,** 395–409.

Guiot, J. (1990) Methodology of the last climatic cycle reconstruction in France from pollen data. *Palaeogeography Palaeoclimatology Palaeoecology*, **80,** 49–69.

Harrison, S.P., Prentice, I.C. & Guiot, J. (1993) Climatic controls of Holocene lake-level changes in Europe. *Climate Dynamics*, **8,** 189–200.

Haxeltine, A. & Prentice, I.C. (1996) BIOME3: an equilibrium terrestrial biosphere model based on ecophysiological constraints, resource availability, and competition among plant functional type. *Global Biogeochemical Cycles*, **10,** 693–709.

Hernandez, M.L., Passas, H.J. & Smith, L.G. (1999) Clonal analysis of epidermal Patterning during maize leaf development. *Developmental Biology*, **216,** 646–658.

Hsiao, T.C., O'Toole, J.C., Yambo, E.B. & Turner, N. (1984) Influence of osmotic adjustment on leaf rolling and tissue death in rice. *Plant Physiology*, **75,** 338–341.

Huang, Y., Dupont, L., Sarnthein, M., Hayes, J.M. & Eglinton, G. (2000) Mapping of C_4 plant input from North West Africa into North East Atlantic sediments. *Geochimica et Cosmochimica Acta*, **64,** 3505–3513.

Hutchinson, J. & Dalziel, J.M. (1968–72) *Flora of west tropical Africa*, 2nd edn, Vol, 3, part 1 and 2 (ed. by R.W.J. Keay). Crown Agents, London, UK.

Jacobs, S.W. (1987) Systematics of the Chloridoid grasses. *Grass systematics and evolution* (ed. by T.R. Soderstrom, K.W. Hilu, C.S. Campell and M.E. Barkworth), pp. 277–286. S.I. Press, Washington, DC.

Jarvis, P.G. & MacNaughton, K.G. (1986) Stomatal control of transpiration: scaling up from leaf to region. *Advanced Ecological research*, **15,** 1–49.

Jolly, D., Prentice, I.C., Bonnefille, R., Ballouche, A., Bengo, M., Brenac, P., Buchet, G., Burney, D., Cazet, J., Cheddadi, R., Edorh, T., Elenga, H., Elmoutaki, S., Guiot, J., Laarif, F., Lamb, H., Lézine, A., Maley, J., Mbenza, M., Peyron, O., Reille, M., Reynaud-Farrera, I., Riollet, G., Ritchie, J., Roche, E. et al. (1998) Biome reconstruction from pollen and plant macrofossil data for Africa and the Arabian peninsula at 0 and 6000 years. *Journal of Biogeography*, **25,** 1007–1027.

Kaplan, L., Smith, M.B. & Sneddon, L.A. (1992) Cereal grain phytoliths of Southwest Asia and Europe. *Phytoliths systematics, emerging issues* (ed. by G.J. Rapp and S.C. Mulholland), pp. 149–174. Advances in Archaeological and Museum Science, New York.

Kelly, E.F. (1990) *Method for extracting opal phytoliths from soil and plant material*. Intern. Rep., Dep. Agron. Colorado State University, Fort Collins.

Kondo, R., Childs, C. & Atkinson, I. (1994) *Opal phytoliths of New Zealand*. Manaaki Whenua Press, Lincoln, Canterbary New Zealand, pp. 85.

Kurmann, M.H. (1985) An opal phytolith and palynomorph study of extant and fossil soils in Kansas (USA). *Palaeogeography, Palaeoclimatology, Palaeoecology*, **49,** 217–235.

Le Cohu, M.-C. (1973) Examen au Microscope Electronique à Balayage des cônes de silice chez les Cypéracées. *Compte rendu de l'académie des sciences, Paris*, **277,** 130–133.

Le Houerou, H.N. (1988) Interannual variability of rainfall and its ecological and managerial consequences on natural vegetation, crops and livestocks. *Time scale and water stress – Proceedings of the 5th International Conference on Mediterranean Ecosystems* (ed. by F. Di Castri, C. Floret, S. Rambal and J. Roy), pp. 323–346. IUBS, Paris.

Le Houérou, H.N. (1993a) Grasslands of the Sahel. *Ecosytems of the World, 8B: Natural grassland* (ed. by R.T. Coupland), pp. 197–220. Elsevier, Amsterdam.

Le Houérou, H.N. (1993b) An overview of the African deserts. *Illustrated library of the earth: Deserts*. Chapter 3.1. Weldon Owen Publishers, Sydney.

Leemans, R. & Cramer, W. (1991) The IIASA database for mean monthly values of temperature, precipitation and

cloudiness of a global terrestrial grid. *International Institut for Applied Systems Analysis (IIASA)*, **RR-91-18,** 61.

Lézine, A.M. (1987) Paléoenvironnements végétaux d'Afrique nord-tropicale depuis 12 000 ans B.P. Analyse pollinique de séries sédimentaires continentales (Sénégal – Mauritanie). Volume I: Texte. Volume II: Annexes. PhD Thesis, Université Aix-Marseille 2 – Faculté des Sciences de Luminy, France, pp. 207.

Lézine, A.M. (1988) New pollen data from the Sahel, Senegal. *Review of Palaeobotany and Palynology*, **55/1–3,** 141–154.

Lézine, A.M. & Edorh, T.M. (1991) Modern pollen deposition in West African Sudanian environments. *Review of Palaeobotany and Palynology*, **67,** 41–58.

Lézine, A.M., Turon, J.L. & Buchet, G. (1995) Pollen analyses of Senegal: evolution of the coastal paleoenvironment during the last deglaciation. *Journal of Quaternary Science*, **10,** 95–105.

Livingstone, D.A. & Clayton, W.D. (1980) An altitudinal cline in tropical African grass floras and its paleoecological significance. *Quaternary Research*, **13,** 392–402.

Moulia, B. (1994) The biomechanics of leaf rolling. *Biomimetics*, **2,** 267–281.

Mulholland, S.C. (1989) Phytoliths shape frequencies in North Dakota grasses: a comparison to general patterns. *Journal of Archaeological Science*, **16,** 489–511.

O'Toole, J.C. & Cruz, T.R. (1980) Response of leaf water potential, stomatal resistance, and leaf rolling to water stress. *Plant physiology*, **65,** 428–432.

Ollendorf, A.L. (1987) Archeological implications of a phytolith study at Tel Miqne (Ekron), Israel. *Journal of Field Archaeology*, **14,** 453–463.

Palmer, P.G., Gerbeth-jones, S. & Hutchison, S. (1985) A scanning electron microscope survey of the epidermis of East African grasses, III. *Smithsonian Contribution to Botany*, Vol. 55. Smithsonian Institution, Washington, DC, pp. 135.

Parry, D.W. & Smithson, F. (1958) Silicification of bulliform cells in grasses. *Nature*, **181,** 1549–1550.

Parton, W.J., Ojima, D.S. & Schimel, D.S. (1994) Environmental change in grasslands: assessment using models. *Climatic Change*, **28,** 111–141.

Peyron, O. (1999) Le climat de l'Europe et de l'Afrique au dernier maximum glaciaire et à l'Holocène moyen. French Thesis, Université de Droit et d'Économie d'Aix-Marseille III, Marseille, pp. 203.

Peyron, O., Jolly, D., Bonnefille, R., Vincens, A. & Guiot, J. (2000) Holocene climate of East Africa. *Quaternary Research*, **54,** 90–101.

Piperno, D.P. (1988) *Phytolith analysis – an archaeological and geological perspective*, Vol. 1. Academic Press/Harcourt Brace Jovanovich, New York, pp. 280.

Piperno, D.R. & Jones, J.G. (2003) Paleoecological and archaeological implications of a Late Pleistocene/Early Holocene record of vegetation and climate from the Pacific coastal plain of Panama. *Quaternary Research*, **59,** 79–87.

Prentice, I.C., Cramer, W., Harrison, S.P., Leemans, R., Monserud, R.A. & Solomon, A.M. (1992) A global biome model based on plant physiology and dominance, soil properties and climate. *Journal of Biogeography*, **19,** 117–134.

Ratmeyer, V., Balzer, W., Bergametti, G., Chiapello, I., Fischer, G. & Wyputta, U. (1999a) Seasonal impact of mineral dust on deep-ocean particule flux in the eastern subtropical Atlantic Ocean. *Marine Geology*, **159,** 241–252.

Ratmeyer, V., Fischer, G. & Wefer, G. (1999b) Lithogenic particle fuxes and grain size distributions in the deep ocean off northwest Africa: Implications for seasonal changes of aeolian dust input and downward transport. *Deep Sea Research Part I*, **46,** 1289–1337.

Rovner, I. (1971) Potential of opal phytoliths for use in paleoecological reconstruction. *Quaternary Research*, **1,** 343–359.

Ruddiman, W.F. (1997) Tropical Atlantic terrigenous fluxes since 25,000 yrs B.P. *Marine Geology*, **136,** 189–207.

Runge, F. (1999) The opal phytolith inventory of soils in central Africa – quantities, shapes, classification, and spectra. *Review of Palaeobotany and Palynology*, **107,** 23–53.

Runge, F. & Fimbel, R. (1999) Opal phytoliths as evidence for the formation of savanna islands in the rain forest of Southeast Cameroon. *Proceeding of the VXth INQUA Conference (15th: 1999: Durban South Africa) – Palaeoecology of Africa and the surrounding islands* (ed. by K. Heine and G.E.J. Runge), pp. 171–189. International Union for Quaternary Research, Tokyo.

Sangster, A.G. & Parry, D.W. (1968) Some factors in relation to bulliform cell silicification in the grass leaf. *Annals of Botany*, **33,** 315–323.

Scott, L. (2002) Grassland development under glacial and interglacial conditions in southern Africa: review of pollen, phytolith and isotope evidence. *Palaeogeography, Palaeoclimatology, Palaeoecology*, **177,** 47–57.

Scurfield, G., Anderson, C.A. & Segnit, E.R. (1974) Silica in woody stems. *Australian Journal of Botany*, **22,** 211–229.

Shields, L.M. (1951) The evolution mechanism in leaves of certain xeric grasses. *Phytomorphology*, **1,** 225–241.

Stephenson, N.L. (1998) Actual evapotranspiration and deficit: biologically meaningful correlates of vegetation distribution across spatial scales. *Journal of Biogeography*, **25,** 855–870.

Sykes, M., Prentice, I.C. & Cramer, W. (1996) A bioclimatic model for the potential distributions of north European tree species under present and future climates. *Journal of Biogeography*, **23,** 203–233.

Teeri, J.A. & Stowe, L.G. (1976) Climatic patterns and the distribution of C_4 grasses in North America. *Oecologia (Berl.)*, **23,** 1–12.

Tieszen, L.L., Senyimba, M.M. & Imbamba, S.K. (1979) The distribution of C_3 and C_4 grasses and carbon isotope discrimination along a altitudinal and moisture gradient in Kenya. *Oecologia*, **37,** 337–350.

Tronchain, J. (1940) *Ecologie végétale de la zone intertropicale*. Univ. Paul Sabatier, Toulouse, pp. 468.

Twiss, P.C. (1992) Predicted world distibution of C3 and C4 grass phytoliths. *Phytolith systematics: emerging issues* (ed. by

G. Rapp, Jr and S.C. Mulholland), pp. 113–128. Advances in Archaeological and Museum Science, vol. 1. Plenum Press, New York.

Twiss, P.C., Suess, E. & Smith, R.M. (1969) Morphological classification of grass phytoliths. *Procedure of Soil Science Society of America*, **33,** 109–115.

Vrydaghs, L. & Doutrelepont, H. (2000) Analyses phytolithariennes: acquis et perspectives. *Dynamiques à long terme des écosystèmes forestiers intertropicaux*. (ed. by S. Servant-Vildary and M. Servant). UNESCO, Paris.

Wallis, L. (2003) An overview of leaf phytolith production patterns in selected northwest Australian flora. *Review of Palaeobotany and Palynology*, **125,** 201–248.

White, F. (1983) *The Vegetation Map of Africa*. UNESCO, Paris, pp. 356.

Wyk, J. (1979) A general account of the grass cover of Africa. *Ecology of Grasslands and Bamboolands in the World*, **1,** 124–132.

Wyputta, U. & Grieger, B. (1999) Comparison of eastern Atlantic atmospheric trajectories for present day and last glacial maximum. *Palaeogeography, Palaeoclimatology, Palaeoecology*, **146,** 53–66.

Zhao, M., Eglinton, G., Haslett, S.K., Jordan, R.W., Sarnthein M. & Zhang, Z. (2000) Marine and terrestrial biomarker records for the last 35,000 years at ODP site 658C off NW Africa. *Organic Geochemistry*, **31,** 919–930.

BIOSKETCHES

Laurent Bremond has recently obtained his doctorate, working on calibrating modern phytolith assemblages with vegetation and climate data. The main grassland communities surveyed were located in West and East Africa, where tree cover density and C_3/C_4 grass dominance were also studied.

Anne Alexandre is a young scientist working at CNRS. Her main research topics are (1) phytoliths, palaeoenviroments and biogeochemical cycling of silicon, and (2) oxygen isotopes composition of biogenic and low temperature-silicates.

Odile Peyron is a CNRS researcher specializing in the quantitative reconstruction of past climatic parameters from pollen data. Her recent studies have focused on Late Glacial and Holocene palaeoclimates in Europe.

Joël Guiot is a CNRS research director at CEREGE. His work is based on vegetation and climate reconstruction in the past and on the impact of global changes on vegetation. He is a member of the scientific committee of PMIP and is a member of the BIOME6000 project.

Editor: Philip Stott